*J. Fluid Mech.* (2004), *vol.* 507, *pp.* 367–379. © 2004 Cambridge University Press 
DOI: 10.1017/S0022112004008791 Printed in the United Kingdom

# Navier–Stokes solutions for parallel flow in rivulets on an inclined plane

By CARLOS A. PERAZZO[1] AND JULIO GRATTON[2]

[1]Universidad Favaloro, Solís 453, 1078, Buenos Aires, Argentina

[2]INFIP CONICET, Dpto. de Física, Facultad de Ciencias Exactas y Naturales, Universidad de Buenos Aires, Ciudad Universitaria, Pab. I, Buenos Aires, Argentina

(Received 11 April 2003 and in revised form 27 January 2004)

We investigate the solutions of the Navier–Stokes equations that describe the steady flow of rivulets down an inclined surface. We find that the shape of the free surface is given by an analytic formula obtained by solving the equation that expresses the condition of static equilibrium under the action of gravity and surface tension, independently of the velocity field and of any assumption concerning the rheology of the liquid. The velocity field is then obtained by solving (in general numerically) a Poisson equation in the domain defined by the cross-section of the rivulet. The isovelocity contours are perpendicular to the free surface. Various properties of the solutions are given as functions of the parameters of the problem. Two special analytic solutions are presented. The exact solutions suggest that the lubrication approximation, frequently employed to investigate problems similar to the present one, predicts reasonably well the global properties of the rivulet provided the static contact angle is not too large.

## 1. Introduction

We investigate a family of exact solutions of the Navier–Stokes equations that describe the steady flow of a rivulet down an incline. Liquid flows over inclined solid surfaces under the action of gravity are an ubiquitous phenomenon that occurs in nature, as in lava flows, the linings of mammalian lungs, tear films in the eye, etc., and in artificial instances such as microchip fabrication, tertiary oil recovery as well as in many coating processes. The theory of these currents is usually developed within the framework of the lubrication approximation. Flows on an horizontal plane have been studied theoretically and in the laboratory by several authors (see for example Huppert 1982*a*; Gratton & Minotti 1990; Diez, Gratton & Gratton 1992; Marino *et al.* 1996). The equations for the same problem but on a general topography have been derived by Buckmaster (1977). In many instances these flows must be investigated numerically (see for example Kondic & Diez 2001; Schwartz 1989; Moyle, Chen & Homsy 1999; Eres, Schwartz & Roy 2000 in connection with the fingering instability).

Exact solutions of the Navier–Stokes equation for flows of this type can be of interest for several reasons. First, they represent fundamental fluid dynamic flows and owing to the uniform validity of exact solutions, the basic phenomena involved can be studied in detail, thus providing a valuable insight that can help in understanding problems of a similar kind. Second, they allow the validity of approximations like the lubrication theory to be tested. Finally the exact solutions serve as standards to check the accuracy of the results of numerical simulations. These points have been

https://doi.org/10.1017/S0022112004008791 Published online by Cambridge University Press

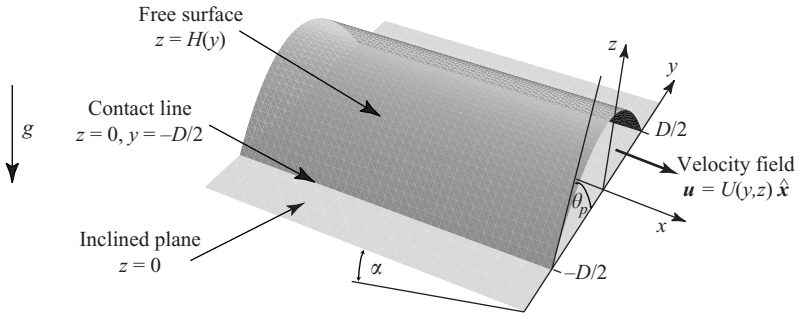



FIGURE 1. Geometry of the problem. A rivulet of width $D$ (only its free surface is shown) is running down an inclined plane forming an angle $\alpha$ with the horizontal. The static contact angle is $\theta_p$ on both sides, and the rivulet is symmetric with respect to the $y=0$ plane. The flow is parallel.

stressed in the review of Wang (1991), in which the reader can find an important list of references that complement the classical treatise of Berker (1963) on exact solutions of the Navier–Stokes equation.

We investigate here steady parallel flows for which the free surface has a shape determined by surface tension and gravity. Surface tension also provides the lateral confinement to a rivulet flowing down an inclined plane. A related problem has been investigated by Scholle & Aksel (2001), who derived exact solutions of the Navier–Stokes equation for the viscous–capillary flow in a rectangular inclined channel, for various meniscus shapes.

From the experimental research of Huppert (1982*b*) and Silvi & Dussan V. (1985) on currents with a moving contact line on an inclined plane, it is well known that an instability occurs leading to the development of a pattern of rivulets called 'fingers'. Owing to its relevance for the technology of various industrial processes, this instability has been intensively studied experimentally, as well as theoretically and numerically within the lubrication approximation (see Kondic & Diez 2001 and references therein). Since under certain conditions the middle part of the fingers consists of an almost parallel flow, we believe that the exact solutions we derive here, that are an improvement on the lubrication approximation, may help to describe better this aspect of the phenomenon.

In § 2 we derive the basic equations, and show that the shape of the free surface does not depend on the velocity field, as it is determined by a static equilibrium condition. In § 3 we obtain analytical formulae for the free surface, for arbitrary values of the parameters of the problem. In § 4 we present the equations that determine the velocity field, and in § 5 we describe two special solutions that can be obtained in closed form. In general, however, the equations of the velocity field must be solved numerically. To this end we employ a finite elements method, and the results are presented in § 6. Then in § 7 we compare our exact solutions with those obtained from the lubrication approximation. Section 8 contains the concluding remarks.

## 2. Basic equations

We consider the steady flow of a rivulet of a Newtonian fluid, running down a plane whose angle of inclination is $\alpha$, as shown in figure 1. We shall assume $0 \leqslant \alpha \leqslant \pi/2$. The coordinate $z$ is perpendicular to the plane, and the $x$, $y$ coordinates lie in the

https://doi.org/10.1017/S0022112004008791 Published online by Cambridge University Press

plane; $y$ is horizontal, and $x$ increases downwards. We assume that the rivulet extends from $-\infty < x < +\infty$, that the velocity of the fluid is $\boldsymbol{u} = U(y,z)\hat{\boldsymbol{x}}$, and that its free surface is given by $H \equiv H(y)$. The rivulet is confined laterally by surface tension so that the width of the wetted strip is $D$, and we assume that the static contact angle $\theta_p$ is the same on both sides. Clearly the rivulet is symmetric with respect to the plane passing through the maximum of $H(y)$. We take the origin of the $y$-coordinate at this plane, so that the wetted strip is $-D/2 < y < D/2$ (notice that if $\theta_p > \pi/2$ the width of the rivulet is larger than $D$). Then $H(y) = H(-y)$, $H'(0) = 0$ (primes denote derivatives of $H$ with respect to $y$) and $U(y,z) = U(-y,z)$.

The continuity equation is clearly satisfied, and the Navier–Stokes equation reduces to

$$p_x = \mu(U_{yy} + U_{zz}) + \rho g \sin\alpha, \tag{2.1}$$

$$p_y = 0, \tag{2.2}$$

$$p_z = -\rho g \cos\alpha, \tag{2.3}$$

where $p$ is the pressure, $\rho$ is the density, $g$ is the acceleration due to gravity, $\mu$ is the viscosity, and we denote the derivatives of $p$ and $U$ with respect to $x$, $y$, $z$ with appropriate suffixes.

The boundary condition at the free surface is

$$\boldsymbol{\sigma} \cdot \hat{\boldsymbol{n}} = \gamma C \hat{\boldsymbol{n}}. \tag{2.4}$$

Here $C = H''(1 + H'^2)^{-3/2}$ denotes the curvature of the free surface, $\gamma$ is the surface tension, $\hat{\boldsymbol{n}}$ is the normal to the free surface of the liquid, given by

$$\hat{\boldsymbol{n}} = \frac{-H'\hat{\boldsymbol{y}} + \hat{\boldsymbol{z}}}{\sqrt{1 + H'^2}}$$

and the components of the stress tensor $\boldsymbol{\sigma}$ are

$$\boldsymbol{\sigma} = \begin{bmatrix} -p & \mu U_y & \mu U_z \\ \mu U_y & -p & 0 \\ \mu U_z & 0 & -p \end{bmatrix}.$$

Equation (2.4) leads to the conditions

$$p = -\gamma C \quad \text{and} \quad U_z = H' U_y \quad \text{at } z = H. \tag{2.5}$$

Integrating (2.3) and using (2.5) we obtain $p = \rho g (H - z)\cos\alpha - \gamma C$, so that the pressure is hydrostatic. Using this result in (2.2) we obtain a differential equation for $H(y)$:

$$kH' = \left[\frac{H''}{(1 + H'^2)^{3/2}}\right]', \tag{2.6}$$

where we have set $k = (\rho g/\gamma)\cos\alpha$ ($k$ is the inverse of the square of the capillary length). Owing to the symmetry of the problem it is sufficient to solve (2.6) for $y \geqslant 0$ subject to the boundary conditions

$$H(D/2) = 0, \quad H'(D/2) = -\tan\theta_p, \quad H'(0) = 0. \tag{2.7}$$

The solution of this problem is independent of $U(y,z)$, since the shape of the free surface is determined by a static equilibrium condition, as the fluid motion is always parallel to the surface. This leads to a great simplification, since $H(y)$ can be calculated first, and the result can then be used as a datum in the equations that determine the

https://doi.org/10.1017/S0022112004008791 Published online by Cambridge University Press

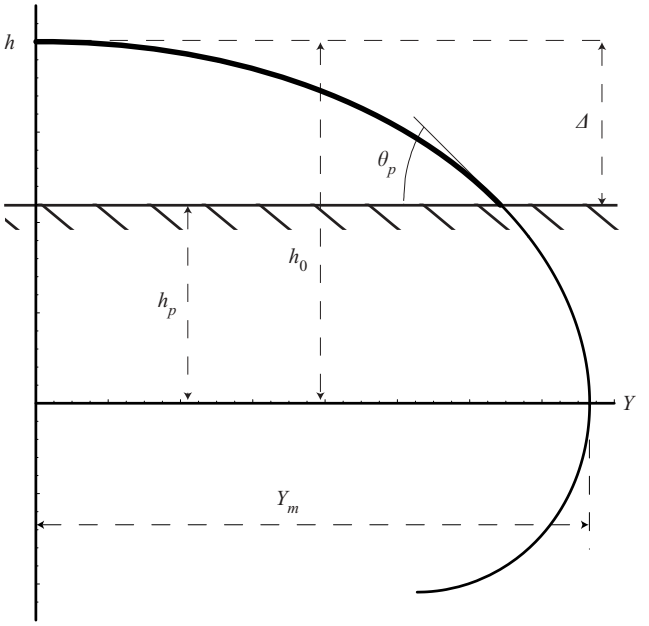



FIGURE 2. Coordinate system employed to describe the free surface. Only the right half is shown since $H(-Y)=H(Y)$. The coordinate perpendicular to the supporting plane (dashed in the figure) is measured from the plane where the slope of the solution of (2.6) takes the value $\theta=\pm\pi/2$. Then, the shape of the free surface is given by the portion of the curve (thick line) lying above $h_p$, where the supporting plane is located so that $H'(Y)=\pm\theta_p$.

velocity field. It can also be noticed that $H(y)$ is independent of the rheology, so that the present treatment can be extended to a non-Newtonian fluid.

The equation for $U$ is

$$U_{yy}+U_{zz}=-\frac{g\sin\alpha}{\nu} \tag{2.8}$$

($\nu=\mu/\rho$) subject to the boundary conditions

$$U(y,0)=0, \quad U_z(y,H)-H'U_y(y,H)=0. \tag{2.9}$$

We observe that if the rivulet is flowing over a non-planar surface whose relief depends only on $y$ and not on $x$ (such as an inclined channel of arbitrary cross-section), we obtain the same equations except that the boundary conditions (2.7) at the contact line and (2.9) at the bottom must be changed according to the relief of the supporting surface.

## 3. The shape of the free surface

The classical study on the shapes of static menisci is due to Bashforth & Adams (1892), and is amply discussed in the monograph by Padday (1969). For discussions of the physics of the static contact line see Dussan V. (1979) and de Gennes (1985). We denote by $Y$, $H$ the coordinates of a point of the free surface. For reasons that will be apparent later, in solving the problem (2.6–2.7) it is convenient to change the origin of the coordinate perpendicular to the supporting plane. Accordingly, we shall employ a vertical coordinate $z'$ such that $z'=0$ is the plane where the slope of the solution of (2.6) takes the value $\theta=\pm\pi/2$ (see figure 2) and $z'=h_p$ is the supporting

https://doi.org/10.1017/S0022112004008791 Published online by Cambridge University Press

plane $z=0$ ($h_p>0$ if $\theta_p<\pi/2$ and $h_p<0$ if $\theta_p>\pi/2$). Then the free surface is given by $h=H+h_p$.

We set $\Delta=H(0)$ and $h_0=\Delta+h_p$ so that (2.6) becomes

$$kh'=\left[\frac{h''}{(1+h'^2)^{3/2}}\right]', \tag{3.1}$$

and (2.7) are converted into

$$h(d/2)=h_p, \quad h'(d/2)=-\tan\theta_p, \quad h'(0)=0.$$

Integrating (3.1) from 0 to $Y$, multiplying by $h'$, and integrating again, we obtain

$$\tfrac{1}{2}k(h-h_0)^2=1-\frac{1}{\sqrt{1+h'^2}}-(h-h_0)h''(0). \tag{3.2}$$

Calling $Y_m$ the value of $Y$ for which $h(Y_m)=0$ and $h'(Y_m)=-\infty$ and using (3.2) we find

$$h''(0)=\tfrac{1}{2}kh_0-\frac{1}{h_0}. \tag{3.3}$$

We observe that $h''(0)$ is the curvature of the free surface at the vertex, which is negative. On the other hand $|h''(0)|$ must be smaller than $h_0^{-1}$ (which corresponds to the circular shape that is achieved when surface tension dominates). Then one finds that

$$0\leqslant\beta\equiv\tfrac{1}{2}kh_0^2\leqslant 1. \tag{3.4}$$

Substituting (3.3) in (3.2) we obtain

$$\frac{h}{h_0}+\tfrac{1}{2}kh(h_0-h)=\frac{1}{\sqrt{1+h'^2}}. \tag{3.5}$$

Introducing the dimensionless variables $\zeta=h/h_0$, $\eta=Y/h_0$, (3.5) takes the form

$$\zeta[1+\beta(1-\zeta)]=\frac{1}{\sqrt{1+(\mathrm{d}\zeta/\mathrm{d}\eta)^2}}.$$

Solving for $\mathrm{d}\eta/\mathrm{d}\zeta$ we obtain

$$\frac{\mathrm{d}\eta}{\mathrm{d}\zeta}=\pm\frac{\zeta[1+\beta(1-\zeta)]}{\sqrt{1-\zeta^2[1+\beta(1-\zeta)]^2}}.$$

For $\beta<1$, this equation can be integrated to find

$$\eta=\pm\left\{\frac{\sqrt{1-\zeta^2[1+\beta(1-\zeta)]^2}}{1-\beta\zeta}+\sqrt{\frac{2}{a\beta}}[F(\phi\mid a^2)-E(\phi\mid a^2)]\right\}. \tag{3.6}$$

Here $F(\phi\mid a^2)$ and $E(\phi\mid a^2)$ are, respectively, the elliptic integrals of the first and second kind (see Abramowitz & Stegun 1970), and we use the notation

$$\phi=\arcsin\left(\sqrt{\frac{\beta(1-\zeta)}{a(1-\beta\zeta)}}\right), \quad a=\frac{\sqrt{1+\beta(6+\beta)}+1-\beta}{\sqrt{1+\beta(6+\beta)}-1+\beta}.$$

Notice that $a>1$. In figure 3 we show $\eta(\zeta)$ for several values of $\beta$; it can be seen that the cross-section of the rivulet tends to become circular as $\beta\to 0$, and becomes flatter

https://doi.org/10.1017/S0022112004008791 Published online by Cambridge University Press

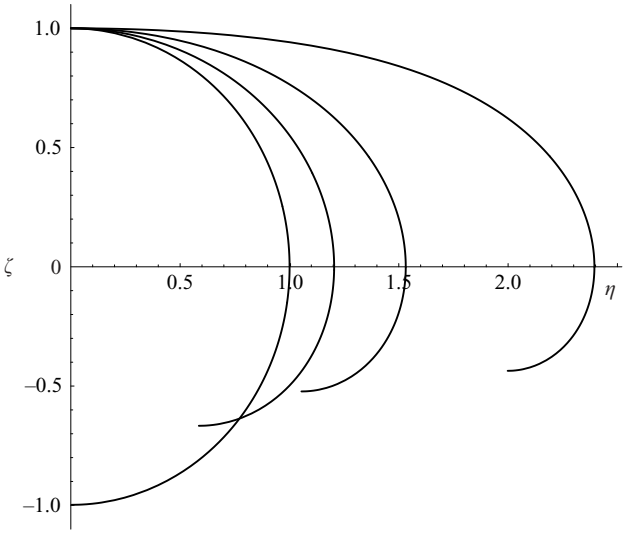



FIGURE 3. The shape of the free surface given by (3.6). From left to right, the values of $\beta$ are 0, 0.3, 0.6 and 0.9.

and wider as $\beta$ increases. In the limit when gravity dominates over surface tension $\beta \to 1$ and $D \to \infty$. The shape of the free surface near the contact line is then given by

$$\tilde{\eta} = \eta - \frac{d}{2} = \sqrt{1+h(2-h)} - 1 - \frac{1}{\sqrt{2}}\left(\operatorname{arctanh}\sqrt{\frac{1+h(2-h)}{2}} - \operatorname{arctanh}\frac{1}{\sqrt{2}}\right)$$

where $\tilde{\eta}$ is measured from the point where the slope of $h$ is vertical and $d = D/h_0$. This solution is related to the cylindrical meniscus of Bashforth & Adams (1892).

It is convenient to express the equation of the free surface using the slope $\theta = \arctan(\mathrm{d}\zeta/\mathrm{d}\eta)$ as a parameter. We obtain

$$\zeta = \frac{1}{2\beta}(1+\beta-\sqrt{(1+\beta)^2-4\beta\cos\theta}), \tag{3.7}$$

$$\eta = \frac{1}{2\beta(1-\beta)}\left\{(1-\beta)^2 E\left(\frac{\theta}{2}\middle| -\frac{8\beta}{(1-\beta)^2}\right) - (1+\beta)^2 F\left(\frac{\theta}{2}\middle| -\frac{8\beta}{(1-\beta)^2}\right)\right\}. \tag{3.8}$$

Now we can appreciate the rationale of our change of the origin of the coordinates: by this device we obtained expressions for $\zeta$ and $\eta$ that depend only on $\beta$, and not on $\theta_p$. The contact angle only determines the position $\zeta_p$ of the supporting plane, given by $\zeta_p = \zeta(\theta_p)$. The dimensionless width of the wetted stripe of the supporting plane is $d = 2\eta_p = 2\eta(\theta_p)$ and we can define the aspect ratio of the rivulet as $R = (1-\zeta_p)/d$.

Of course $\beta$ depends on $h_0$, which is not directly observed in the actual profile. For this reason we need formulae that relate $h_0$ and $\beta$ to some quantity easily compared to the visible shape of the rivulet, such as its maximum thickness $\Delta$. Defining

$$\lambda = \frac{1}{2}k\Delta^2 = \frac{\rho g\cos\alpha}{2\gamma}\Delta^2$$

https://doi.org/10.1017/S0022112004008791 Published online by Cambridge University Press

we find $h_0 = \delta\Delta$ with

$$\delta = \frac{1}{2\lambda}\left(\lambda - 1 + \cos\theta_p + \sqrt{(\lambda - 1 + \cos\theta_p)^2 + 4\lambda}\right), \quad \beta = 1 + \delta(\lambda - 1 + \cos\theta_p),$$

which are the desired formulae. Notice that the condition (3.4) is equivalent to the static equilibrium condition

$$\lambda = \tfrac{1}{2}k\Delta^2 \leqslant 1 - \cos\theta_p,$$

which sets the upper limit to the thickness of the rivulet.

## 4. The velocity field

We now turn to the calculation of the velocity field. We introduce $t = z/h_0$, $s = y/h_0$, $u = U/U_0$ where $U_0 = \nu^{-1}h_0^2 g\sin\alpha$, so that (2.8) becomes the Poisson equation

$$u_{ss} + u_{tt} = -1, \tag{4.1}$$

and the boundary conditions (2.9) are now

$$u(s, \zeta_p) = 0, \quad u_t(s, \zeta) - \frac{\mathrm{d}\zeta}{\mathrm{d}\eta}u_s(s, \zeta) = 0. \tag{4.2}$$

It can be easily verified that the last condition implies that the lines of equal velocity are always perpendicular to the free surface. Notice that owing to the elliptic nature of the problem for the velocity field, the discontinuity in the boundary condition (at the contact line) does not lead to a discontinuity in the interior of the flow domain.

In general the problem (4.1)–(4.2) must be solved numerically. Before discussing the results, we show two special solutions that can be obtained in closed form and comment on their properties.

## 5. Special analytic solutions

When surface tension dominates the shape of the rivulet (as happens when the supporting plane is nearly vertical) we have $\beta = 0$, and the cross-section is a circular segment. If in addition $\theta_p$ is $\pi/2$ or $\pi$ it is possible to obtain the solution in closed form.

### 5.1. *The solution for* $\beta = 0$, $\theta_p = \pi/2$

Equation (4.1) can be reduced to Laplace equation by setting

$$u = -\tfrac{1}{2}(t - \zeta_p)^2 + \tilde{u}, \tag{5.1}$$

thus obtaining

$$\tilde{u}_{ss} + \tilde{u}_{tt} = 0. \tag{5.2}$$

The boundary conditions that $\tilde{u}$ must satisfy are

$$\tilde{u}(s, \zeta_p) = 0, \quad \tilde{u}_t(s, \zeta) - \frac{\mathrm{d}\zeta}{\mathrm{d}\eta}\tilde{u}_s(s, \zeta) = \zeta - \zeta_p. \tag{5.3}$$

We use polar coordinates $r, \theta$; then $s = r\cos\theta$, $t = r\sin\theta$, the free surface is $r = 1$ ($\eta = \cos\theta$, $\zeta = \sin\theta$, $0 \leqslant \theta \leqslant \pi$) and $\mathrm{d}\zeta/\mathrm{d}\eta = -\cot\theta$. The condition (5.3) is then

$$\tilde{u}_r(1, \theta) = \sin^2\theta, \quad 0 \leqslant \theta \leqslant \pi, \tag{5.4}$$

https://doi.org/10.1017/S0022112004008791 Published online by Cambridge University Press

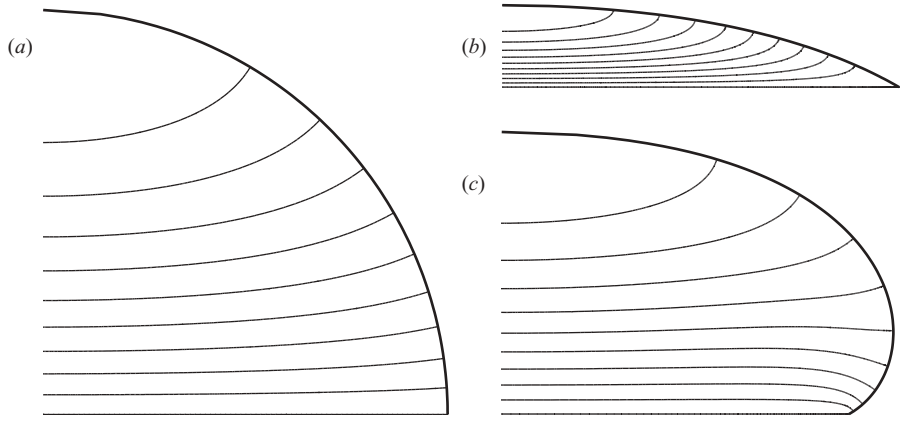



FIGURE 4. Contour plots of (*a*) the solution (5.9), (*b*) and (*c*) the numerical solutions of (4.1) and (4.2) for $\beta = 0.8$ and $\theta_p = \pi/6$ and $\theta_p = 5\pi/6$, respectively. The thick line is the free surface, and the thin lines are lines with constant velocity, whose values are equally spaced.

and we have in addition

$$\tilde{u}(r, 0) = \tilde{u}(r, \pi) = 0. \tag{5.5}$$

We first solve (5.2) in the semicircular domain $0 \leqslant r \leqslant 1$, $0 \leqslant \theta \leqslant \pi$ by separation of variables. The solutions that are regular at $r = 0$ and satisfy (5.5) can be expressed as

$$\tilde{u} = \sum_{m=1}^{\infty} a_m r^m \sin m\theta. \tag{5.6}$$

Using the condition (5.4) we find the coefficients of this series as

$$a_m = -\frac{8}{\pi} \frac{1}{m^2(m^2 - 4)} \ (m \text{ odd}), \quad a_m = 0 \ (m \text{ even}). \tag{5.7}$$

Introducing (5.7) in (5.6) we find

$$\tilde{u} = -\frac{8}{\pi} \sum_{n=0}^{\infty} \frac{r^{2n+1} \sin[(2n+1)\theta]}{(2n-1)(2n+1)^2(2n+3)}. \tag{5.8}$$

This series can be expressed in terms of the Lerch trascendent function $\Phi\left(r^2 \mathrm{e}^{2\mathrm{i}\theta}, 2, \frac{1}{2}\right)$ (see Bateman 1953). However, in the calculations it is better to use the expression (5.8). The full solution is obtained using (5.1) as

$$u = -\tfrac{1}{2}t^2 + \tilde{u}. \tag{5.9}$$

The maximum value of $u$ is

$$u(1, \pi/2) = \frac{1 + 2C^*}{\pi} - \frac{1}{2} = 0.401432\ldots,$$

where $C^* = 0.915966\ldots$ is Catalan's constant (see Abramowitz & Stegun 1970). Contour plots of this solutions can be seen in figure 4(*a*).

Integrating (5.9) over the cross-section of the rivulet we obtain the volumetric flow as

$$Q = q \frac{g h_0^4 \sin\alpha}{\nu}, \quad q = \frac{6 - \pi^2 + 7\varsigma(3)}{4\pi} \cong 0.361663\ldots.$$

https://doi.org/10.1017/S0022112004008791 Published online by Cambridge University Press

In this equation $\varsigma$ denotes Riemann's Zeta function (see Abramowitz & Stegun 1970).

### 5.2. *The solution for* $\beta = 0$, $\theta_p = \pi$

It can be verified that the solution of (4.1) that satisfies (4.2) is

$$u = \text{const.} - \tfrac{1}{4}(2 + r^2) + \tfrac{1}{2}\ln(1 + r^2 + 2r\sin\theta),$$

where the constant must be chosen to satisfy (4.2). This solution diverges, as must be expected since for $\beta = 0$, $\theta_p = \pi$ the rivulet touches the supporting plane along a line.

## 6. Numerical solutions

We have not been able to find other closed form solutions in addition to those described above. For arbitrary $\beta$ and $\theta_p$ the velocity field must be calculated numerically. We have used a finite element method to integrate (4.1) subject to the boundary conditions (4.2). The mesh varied from 9000 to 70 000 points according to the shape of the contour. We checked the accuracy of the method by comparing the numerical solution for $\beta = 0$, $\theta_p = \pi/2$ with the closed form solution (5.9). The average difference between the numerical and the exact $u$ was $\approx 0.0015\%$ and the maximum difference was $\approx 0.05\%$.

We calculated solutions for ten values of $\beta$ from 0 to 0.9 and six values of $\theta_p$ from $\pi/6$ to $\pi$. In figure 4$(b, c)$ we show typical contour plots of $u(s, t)$. Notice that the larger velocity gradients occur as expected near the supporting plane and not too close to the surface of the rivulet, where the isovelocity contours are nearly parallel to the plane. On approaching the free surface the isovelocity contours fan out to become perpendicular to the surface.

In figure 5 we represent the dimensionless area $s = S/h_0^2$ of the cross-section of the rivulet, the dimensionless volumetric flow $q = \int u\,\mathrm{d}s$ and the average velocity $\bar{u} = q/s$ (in these figures, the curves joining the calculated points have been obtained by means of spline interpolations). In terms of these quantities and of the geometrical properties of the free surface derived in § 3 any other magnitude of interest can be computed. For example in figure 5 we show the drag coefficient $C = F_x/\frac{1}{2}\rho U^2 D$ ($F_x$ is the drag force per unit length along the rivulet), which can be expressed as

$$C = \frac{s}{\frac{1}{2}d\bar{u}^2}\frac{\nu^2}{h_0^3 g\sin\alpha}.$$

## 7. Comparison with the lubrication approximation

The lubrication approximation (which for brevity we shall denote by LA) is extremely useful and widely used both in theory as in numerical codes owing to its simplicity. It may be interesting to compare the results of the LA with the present exact solutions. Here we shall only give an example, as a systematic investigation of the accuracy of the LA is beyond the scope of this paper.

The basic assumption of the LA (see for example Acheson 1990) is that the free surface is almost parallel to the supporting plane, so that the component of the velocity normal to the plane can be neglected. In the present context this has two consequences. First, the shape of the free surface as given by the LA differs from the exact shape since $H'^2$ is neglected in (2.6), and one obtains

$$\zeta_{LA} = 1 - A\frac{1-\beta}{2}[1 - \cosh(\eta\sqrt{2\beta})], \quad A = \text{const.} \tag{7.1}$$

https://doi.org/10.1017/S0022112004008791 Published online by Cambridge University Press

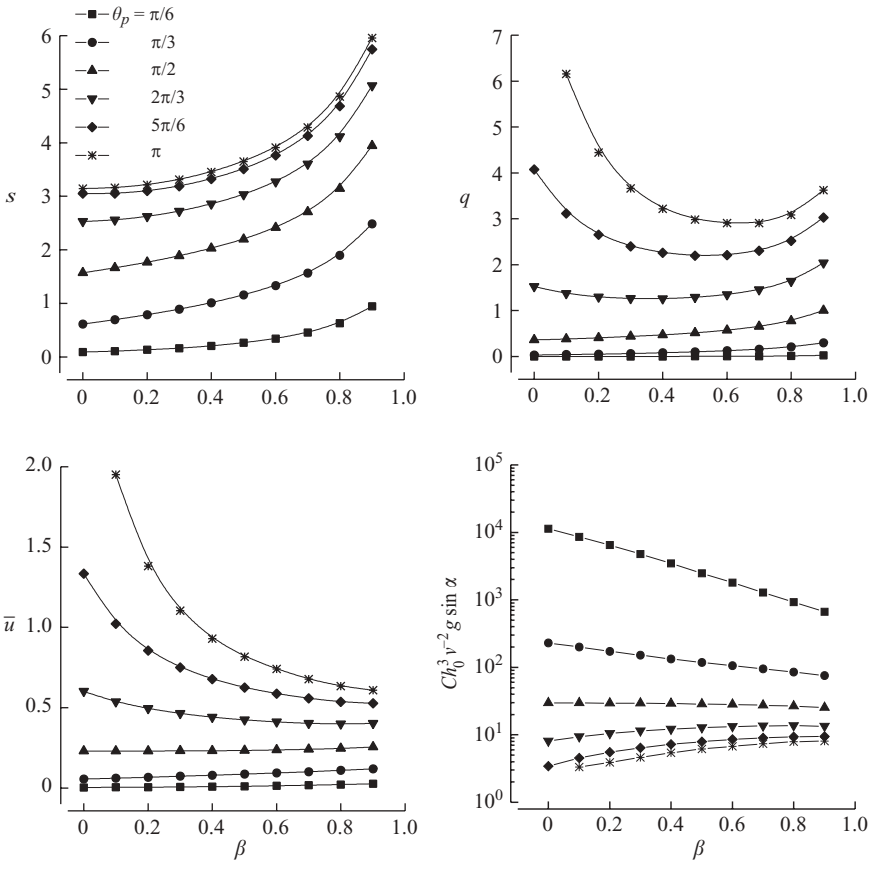



FIGURE 5. The area $s$ of the cross-section, the volumetric flow $q$, the average $u$ and the drag coefficient $C$, all of them as functions of $\beta$ for constant $\theta_p$.

Clearly, (7.1) will not reproduce correctly the shape of the free surface when $\theta_p$ is large, and utterly fails for $\theta_p \geqslant \pi/2$ (like in figure 4$a,c$).

Second, the component $\sigma_{xy}$ of the stress tensor is neglected, and in consequence the velocity field is given by

$$u_{LA}(s,t) = (t - \zeta_p)(\zeta - t/2 - \zeta_p/2) \quad (\zeta = \zeta(s)), \tag{7.2}$$

so that $u_{LA}$ depends only on the local thickness of the current $\zeta(s)$.

To appreciate the effect of the lack of accuracy of $\zeta_{LA}$ we compare in table 1 the exact solution for $\beta = 0.8$ and $\theta_p = 30^\circ$ with the results of the LA for three different values of $A$ corresponding to the three following cases: (i) the exact $\theta_p$ and $\eta_p$, (ii) the exact $\theta_p$ and $\zeta_p$ and (iii) the exact $\zeta_p$ and $\eta_p$. In figure 6($a$) we show $\zeta_{LA}$ for cases (i) and (ii).

The difference between $u_{LA}(s,t)$ (computed using in (7.2) the exact $\zeta(\eta)$ given implicitly by (3.6)) and the exact velocity field can be seen in figure 6($b$) for $\beta = 0.8$ and $\theta_p = 30^\circ$ and in figure 6($c$) for $\beta = 0$ and $\theta_p = 90^\circ$.

It can be seen in table 1 that the global properties of the rivulet ($s$, $q$ and $\bar{u}$) are predicted quite accurately by the LA in case (iii), since even for a contact angle as large as 30° they agree with the exact results to within a few percent. However, the details of the velocity field are not reproduced with the same accuracy: it can be seen

https://doi.org/10.1017/S0022112004008791 Published online by Cambridge University Press

| | $A$ | $\theta_p$ (deg.) | $\eta_p$ | $\zeta_p$ | $s$ | $q$ | $\bar{u}$ |
|---|---|---|---|---|---|---|---|
| Lubrication approximation (i) | 1.4604 | 30 | 1.4684 | 0.6668 | 0.6857 | 0.0180 | 0.0263 |
| Lubrication approximation (ii) | 1.9246 | 30 | 1.2637 | 0.6971 | 0.5323 | 0.0134 | 0.0215 |
| Lubrication approximation (iii) | 1.3276 | 27.7 | 1.4684 | 0.6971 | 0.6234 | 0.0136 | 0.0217 |
| Exact solution | – | 30 | 1.4684 | 0.6971 | 0.6314 | 0.0136 | 0.0216 |

TABLE 1. Comparison of the results of the lubrication approximation with the exact solution for $\beta = 0.8$ and $\theta_p = 30°$.

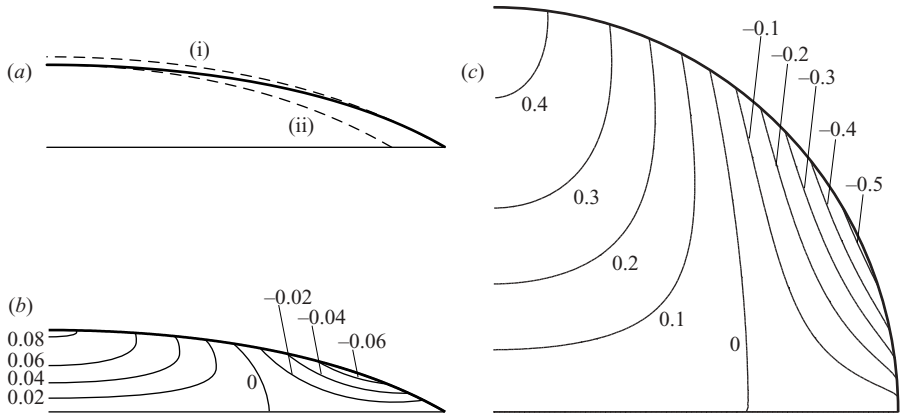



FIGURE 6. Comparison between the exact solution and the results from the lubrication approximation. (*a*) The shape of the free surface; the thick line corresponds to the exact solution for $\beta = 0.8$ and $\theta_p = \pi/6$, the dashed lines correspond to cases (i) and (ii) of table 1 (case (iii) is not shown as in this scale it cannot be distinguished from the exact solution). (*b*, *c*) Comparison of the exact velocity field $u(s,t)$ with $u_{LA}(s,t)$ for $\beta = 0.8$, $\theta_p = \pi/6$ and $\beta = 0$, $\theta_p = \pi/2$, respectively; contour plots of $(u_{LA} - u)/\bar{u}$ are shown.

from figure 6(*b*) that if one uses (7.2) with the exact $\zeta(\eta)$, the LA overestimates the velocity in the central region of the rivulet and underestimates it in its periphery. This happens because $\sigma_{xy}$ (neglected in the LA) transfers momentum from the central part to the sides, and finally to the periphery of the rivulet. This implies a redistribution of momentum, but not a change in its total value, which explains why the inaccuracy of $u_{LA}$ tends to cancel out when computing $\bar{u}$. For example, in this case one obtains $\bar{u} = 0.0219$, very close to the exact result $\bar{u} = 0.0216$. This cancellation can also be appreciated for $\beta = 0$, $\theta_p = 90°$ as shown in figure 6(*c*); in this case the inaccuracy of the velocity field is much larger than in the previous example, as expected because we are considering a situation in which the LA cannot be good. However, using the parabolic profile (7.2) we obtain $\bar{u} = 0.25$, which still is not too far from the exact value $\bar{u} = 0.23$.

## 8. Conclusion

We derived exact solutions of the Navier–Stokes equations that describe the steady parallel flow of rivulets down an inclined surface. The assumption that the flow is parallel decouples the problem of finding the shape of the free surface (which is determined by the static equilibrium under the action of gravity and surface tension

https://doi.org/10.1017/S0022112004008791 Published online by Cambridge University Press

that confines the rivulet laterally) from that of calculating the velocity field, so that the latter can be solved once the free surface is known. Excepting a few special cases, the velocity field must be obtained numerically. We have done this for several values of the parameters $\beta$ and $\theta_p$ and we calculated various global properties (area of the cross-section, volumetric flow, average velocity and drag coefficient) of the rivulet.

We compared our exact solution for $\beta = 0.8$ and $\theta_p = \pi/6$ with the result obtained using the lubrication approximation. We find that the global properties are predicted quite accurately by the lubrication approximation. However, the velocity field as calculated by means of it is not as accurate, overestimating the velocity in the central region of the rivulet and underestimating it in its periphery. We also compared the exact average velocity for $\beta = 0$ and $\theta_p = \pi/2$ with that obtained for the same shape, but using the parabolic vertical velocity profile (7.2) of the lubrication approximation, and find that the difference is not very large. This implies that the errors of the velocity field (7.2) tend to cancel out on averaging over the cross-section, as can be expected for physical reasons.

The present solutions are valid for arbitrary values of the Reynolds number of the flow. However, the issue of their stability remains to be investigated in the future.

We acknowledge grants PIP 02230 of CONICET and X151 of the University of Buenos Aires.

## REFERENCES

Abramowitz, M. & Stegun, I. C. 1970 *Handbook of Mathematical Functions*, 9th printing, Dover.

Acheson, D. J. 1990 *Elementary Fluid Dynamics*. Clarendon.

Bashforth, F. & Adams, J. C. 1892 *An Attempt to Test the Theory of Capillary Action*. Cambridge University Press and Deighton, Bell & Co.

Bateman, H. 1953 *Higher Transcendental Functions*, Vol. 1. McGraw-Hill Book.

Berker, R. 1963 Intégration des équations du mouvement d'un fluide visqueux incompressible. In *Handbuch der Physik VIII/2* (ed. S. Flugge) pp. 1–384, Springer.

Buckmaster, J. 1977 Viscous sheets advancing over dry beds. *J. Fluid Mech.* **81**, 735–756.

Diez, J. A., Gratton, R. & Gratton, J. 1992 Self-similar solution of the second kind for a convergent viscous gravity current. *Phys. Fluids* A **4**, 1148–1155.

Dussan V., E. B. 1979 On the spreading of liquids on solid surfaces: static and dynamic contact lines. *Annu. Rev. Fluid Mech.* **11**, 371–400.

Eres, M. H., Schwartz, L. W. & Roy, R. V. 2000 Fingering phenomena for driven coating films. *Phys. Fluids* **12**, 1278–1295.

de Gennes, P. G. 1985 Wetting: statics and dynamics. *Rev. Mod. Phys.* **57**, 827–863.

Gratton, J. & Minotti, F. 1990 Self-similar viscous gravity currents: phase-plane formalism. *J. Fluid Mech.* **210**, 155–182.

Huppert, H. E. 1982*a* The propagation of two-dimensional and axisymmetric viscous gravity currents over a rigid horizontal surface. *J. Fluid Mech.* **121**, 43–58.

Huppert, H. E. 1982*b* Flow and instability of a viscous current down a slope. *Nature* **300**, 427–429.

Kondic, L. & Diez, J. A. 2001 Pattern formation in the flow of thin films down an incline: Constant flux configuration. *Phys. Fluids* **13**, 3168–3184.

Marino, B. M., Thomas, L. P., Gratton, R., Diez, J. A., Betelú, S. & Gratton, J. 1996 Waiting-time solutions of a nonlinear diffusion equation: Experimental study of a creeping flow near a waiting front. *Phys. Rev.* E **54**, 2628–2636.

Moyle, D. T., Chen, M. S. & Homsy, G. M. 1999 Nonlinear rivulet dynamics during unstable dynamic wetting flows. *Intl J. Multiphase Flow* **25**, 1243–1263.

Padday, J. F. 1969 Theory of surface tension. In *Surface and Colloid Science* (ed. E. Matijevic), **1**, pp. 39–251, Wiley.

https://doi.org/10.1017/S0022112004008791 Published online by Cambridge University Press

Scholle, M. & Aksel, N. 2001 An exact solution of visco-capillary flow in an inclined channel. *Z. Angew. Math. Phys.* **52**, 749–769.

Schwartz, L. W. 1989 Viscous flows down an inclined plane: instability and finger formation. *Phys. Fluids* A **1**, 443–445.

Silvi, N. & Dussan V., E. B. 1985 On the rewetting of an inclined solid surface by a liquid. *Phys. Fluids* **28**, 5–7.

Wang, C. Y. 1991 Exact solutions of the steady-state Navier-Stokes equations. *Annu. Rev. Fluid Mech.* **23**, 159–177.

https://doi.org/10.1017/S0022112004008791 Published online by Cambridge University Press